



THE UNIVERSITY  
*of*  
**WISCONSIN**  
MADISON

# MICROFLUIDIC POINT OF CARE DEVICE FOR MALARIA DIAGNOSIS IN ETHIOPIA

---

FINAL REPORT

*BME 200-300*

**Client: Dr. Timothy Kwa<sup>1</sup>**

**Co-Clients: Dr. Padraic Casserly<sup>1</sup>, Dr. Amit Nimunkar<sup>2</sup>**

**Advisor: Dr. John Puccinelli<sup>2</sup>**

**Co-Advisor: Dr. Christa Wille<sup>2</sup>**

<sup>1</sup>Jimma University; <sup>2</sup>Department of Biomedical Engineering, University of Wisconsin - Madison

Team Roles: Hunter Johnson (Team Leader), Austin Feeney (Communicator), James Jorgensen (BWIG), Zachary Hite (BSAC), Joshua Liberko (BPAG)

12/14/2016

## ABSTRACT

Malaria is one of the most severe parasitic diseases in the world with an estimated 438,000 deaths annually. Although malaria can be treated, the disease is extremely devastating in developing countries, primarily due to lack of timely and accurate diagnosis. Developing countries, such as Ethiopia, have fewer resources and laboratory infrastructure. This prolongs treatment times and increases the economic burden to diagnose and treat the disease. Although malaria prevalence has decreased in the last decade due to increased research interest, the current point of care devices used in rural areas today could greatly improve on specificity, availability, and cost. The creation of an innovative microfluidic point of care device for faster and more accessible malaria diagnosis could save thousands of lives each year. This design aims to utilize the contrasting magnetic characteristics of infected red blood cells in its approach to concentrate infected red blood cells for easier detection and diagnosis. After separation of infected red blood cells, a lateral-flow immunoassay method will be paired with gold nanoparticles to detect and differentiate between the four major strains of the malarial parasite. The integrated separation and detection design is ideal for concentrating infected red blood cells and diagnosing all strains of the disease at the earliest possible time point. Based on the calculated results, the final design takes less than one hour to complete and shows that the 50, 80 and 100  $\mu\text{m}$  constriction point designs are feasible for use.



## TABLE OF CONTENTS

Introduction .....	3
Project Motivation .....	3
Background Information.....	3
Problem Statement.....	5
Specifications.....	5
Client Information .....	5
Preliminary Designs.....	5
Separation Design.....	6
A) Separation: Design Idea One – Cell Deformability.....	6
B) Separation: Design Idea Two – Magnetism .....	6
C) Separation: Design Idea Three – Electrical .....	7
Detection Methods.....	8
D) Detection 1: Design Idea One – BinaxNOW.....	8
E) Detection 2: Design Idea Two - Polystyrene Beads .....	8
F) Detection 3: Design Idea Three – Gold Nanoparticles.....	9
Preliminary Design Evaluation:.....	10
Design Matrix Evaluation.....	11
Proposed Final Design.....	12
Fabrication/Development Process: .....	12
Materials .....	12
Methods .....	12
Final Prototype.....	15
Testing .....	17
Results .....	20
Flow Rate Testing.....	20
Magnetic Separation .....	22
Discussion.....	22
Conclusions .....	24
Acknowledgements.....	24
References .....	25
Appendices .....	28

## INTRODUCTION

### Project Motivation

Infectious diseases continue to plague the developing world as there is a basic lack of diagnostic testing to identify these devastating diseases [1]. Many harmful diseases are treatable but continue to spread due to the lack of a timely diagnosis. One such disease that continues to be one of the main causes of death in the world today is malaria. Nearly half of the world's population, around 3.2 billion people, live in areas at risk of contracting malaria [2]. In 2016, over 200 million cases of malaria are reported each year, with an estimated 438,000 malaria related deaths. Though malaria incidence and mortality have both decreased significantly in the last 15 years, this disease continues to be a global burden and requires immediate attention. A specific, effective, cheap, and easily administered malaria diagnostic test could save thousands of lives and prevent millions of misdiagnosed treatments per year [2]. According to the World Health Organization, diagnostic devices for developing countries should be affordable, sensitive, specific, user-friendly, rapid, equipment free, and delivered to those with the greatest need.

### Background Information

Malaria is caused by a genus of parasites known as *Plasmodium* with four main species: *P. falciparum*, *P. malariae*, *P. ovale*, and *P. vivax*. As the most prevalent, *P. falciparum* and *P. vivax* possess the greatest threat [3]. The malaria life cycle involves two stages within two different organisms, the *Anopheles* mosquito and humans. In mosquitos, the sporogenic cycle occurs, where it matures inside the salivary glands until the mosquito inoculates the sporozoites into the human host. From there the sporozoites infect liver cells and mature into schizonts, which rupture and release merozoites, fully mature parasites, into the bloodstream. The parasite then undergoes asexual proliferation in the erythrocytes, continually infecting and rupturing red blood cells (RBC), which then are responsible for the clinical manifestations of the disease. Once RBCs are infected (iRBC), they express specific antigens indicative of the disease, such as histidine-rich protein 2 (HRP2) or pan-malaria antigen. The cells also exhibit different cell membrane properties, increase in electrical conductivity, and increased magnetic properties [3]. The image below depicts the malaria parasite life cycle (Figure 1).

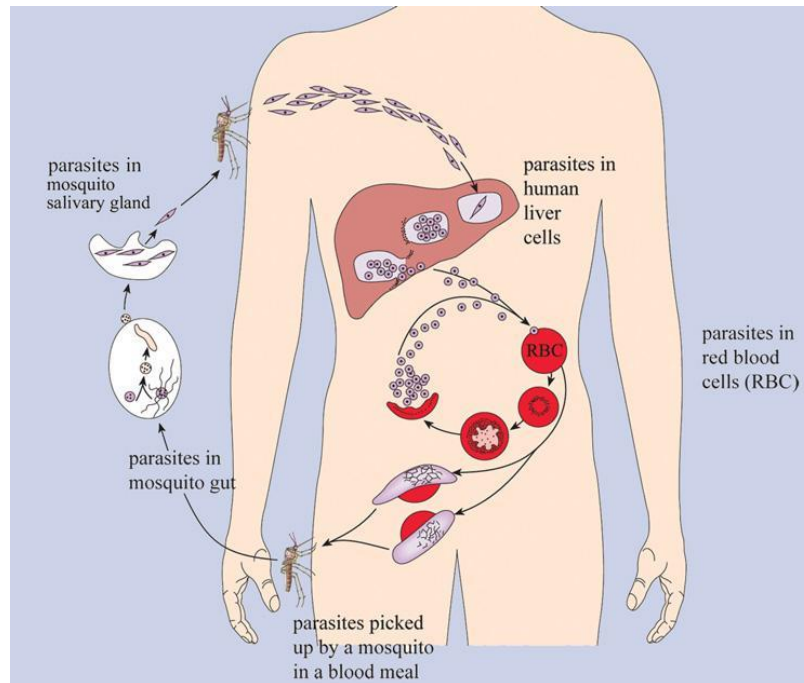


**Figure 1:** Diagram of malaria parasite life cycle. The parasite is transferred to a human through a mosquito bite. It matures in the liver and is then released into the bloodstream where it is later picked up by another mosquito. [http://www.open.edu/openlearnworks/mod/oucontent/view.php?id=88&extra=thumbnail\\_idm37423056](http://www.open.edu/openlearnworks/mod/oucontent/view.php?id=88&extra=thumbnail_idm37423056)

The main method, and gold standard, of malaria detection involves a blood smear visualization of the actual parasite in iRBCs through a microscope. The most common detection is a Giemsa stain, which colors the nuclei of the parasites. Though this method is cheap and extremely effective, it requires a microscope and a trained technician [1]. An alternative and expanding field of research focused on malaria diagnosis today encompasses the development of point of care (POC) testing devices [4]. This approach utilizes both nanotechnology and microfluidics in the development of portable, compact and effective micro platforms for disease testing and diagnosis. These devices allow diagnosis without the use of clinics and give timely diagnostic information. Although saliva and excrement can be used in diagnostic tools, blood is typically used as the input method [4]. Two main types of POC devices in use today include dipsticks and lateral flow tests. Dipsticks detect the presence of simple compounds whereas lateral flow tests rely on immunoassays to detect specific analytes in the specimen via antibody-antigen chemistry [4].

The most accurate POC microfluidic malaria diagnostic device available today is BinaxNOW® by Alere [5]. The paper based test utilizes an immunochromatographic assay for the qualitative detection of *Plasmodium* antigens found in iRBCs of individuals with malaria. It is used for the diagnosis of human malaria, being a rapid, easily administered and interpreted test, as well as having 93.5-99.7% sensitivity for detection of all four strains of malaria, however, it is unable to distinguish between them. Additionally, this is a costly test for the developing

world (~\$40/test). Other issues regarding this test are its inability to distinguish between the four strains of malaria, need for negative result confirmation via smear microscopy, and the requirement for parasite levels to reach 5,000 parasites/ $\mu$ L, a number already associated with severe malaria with clinically perceived symptoms. Although the strains appear to have similar physical effects on a patient, it is important to be able to distinguish between them as the treatment methods vary [3].

### Problem Statement

Due to these shortcomings and the current need for POC testing, the design team was tasked with developing a simple device to diagnose malaria in rural areas in a highly specific, rapid, inexpensive, and replicable manner.

### Specifications

The focused area of this study is Ethiopia, Africa, and the developing world affected by malaria. Ethiopia is a developing country, with limited resources, unreliable internet, little to no qualified laboratory infrastructure/personnel, and predominantly rural areas. Thus, such factors must be considered when designing and fabricating the device. The device also must be 95% accurate, return results within an hour, small in size, under \$5 a test, and able to distinguish between the four strains of malaria, to diagnose the disease.

For more information, related to the design specifications, reference the Product Design Specification (PDS), located in appendix A.

### Client Information

The client is Dr. Timothy Kwa, a professor at Jimma University. Dr. Kwa received his PhD from UC-Davis in Biomedical Engineering and his research interests include improving healthcare through early diagnosis technology. Dr. Padraic Casserly, an associate professor at Jimma University, received his PhD from UW-Madison in Biomedical Engineering and is working with Dr. Kwa to develop the masters program at Jimma University. The BME department was added two years ago and this design project may serve as a thesis for one of the students.

## **PRELIMINARY DESIGNS**

The design of the device consists of two major components. The first aspect of the design will separate iRBCs from normal RBCs based on unique physical characteristics that iRBCs exhibit, while the second aspect will detect if the cells are indeed infected. The separation component operates by concentrating the iRBCs for easier detection. The second component of the design operates by detecting the malarial parasite from the concentrated sample of iRBCs. Preliminary designs for both the separation and detection methods are shown below.

## Separation Design

### *A) Separation: Design Idea One – Cell Deformability*

This separation design is based on changes in cell deformability caused to the host RBCs upon infection with the malarial parasite. Parasitic proteins are secreted within the iRBC to make its membrane more adhesive and stiffer. The increased stiffness leads to a reduction in the surface area to volume ratio which contributes to a significant decrease in cell deformability, especially in late stage iRBCs. Normal RBCs, however, remain highly deformable. It has been demonstrated that the stiffer iRBCs can separate towards the sidewalls of a long and straight channel microfluidic device [6]. The deformable RBCs flowing through the middle of the channel push the rigid iRBCs against the side walls, and with proper side wall placement, create a separation between the iRBCs and RBCs. The diagram below illustrates the preliminary cell deformability design (Figure 2). It has an inlet, where a blood sample is loaded via a syringe. The blood cells then flow down the 3-centimeter-long channel (15  $\mu\text{m}$  wide), which forces the iRBCs to the sidewalls. Finally, the iRBCs can be concentrated in separate outlet from the RBCs via the use of smaller side channels on the outside walls. The innermost outlet would thus mostly contain RBCs, and the outer would contain mostly iRBCs.

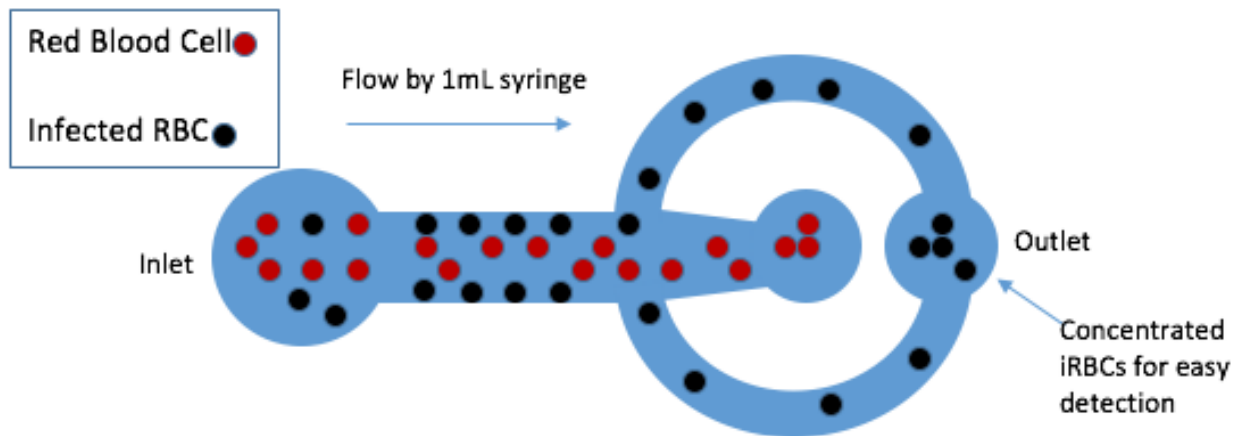


**Figure 2:** This microfluidic device acts in separation of iRBCs from RBCs on the basis of cell deformability characteristics.

### *B) Separation: Design Idea Two – Magnetism*

This separation design is based on changes in magnetic properties of the host RBCs upon infection with the malarial parasite. When parasites infect a cell, they metabolize the hemoglobin of RBCs in order to survive and proliferate. This process releases heme as a toxic byproduct. Heme is then converted into a non-toxic secondary byproduct known as hemozoin. Hemozoin is a weakly paramagnetic crystallite, which is produced during all life stages by all four strains of

the disease [7]. Normal RBCs are diamagnetic, meaning when exposed to a strong magnetic field they will align in the opposite directions. Utilizing different magnetic properties of iRBCs and normal RBCs, the two types can be separated in a highly specific manner in a microfluidic device exposed to properly aligned magnetic fields. Shown below is a preliminary design for magnetic separation of iRBCs involving neodymium magnets (Figure 3) [7][8]. The angle between the separating channels and magnet placement could be tested to determine which angle and which placement would allow for the most consistent flow rate and the best separation between iRBCs and RBCs.

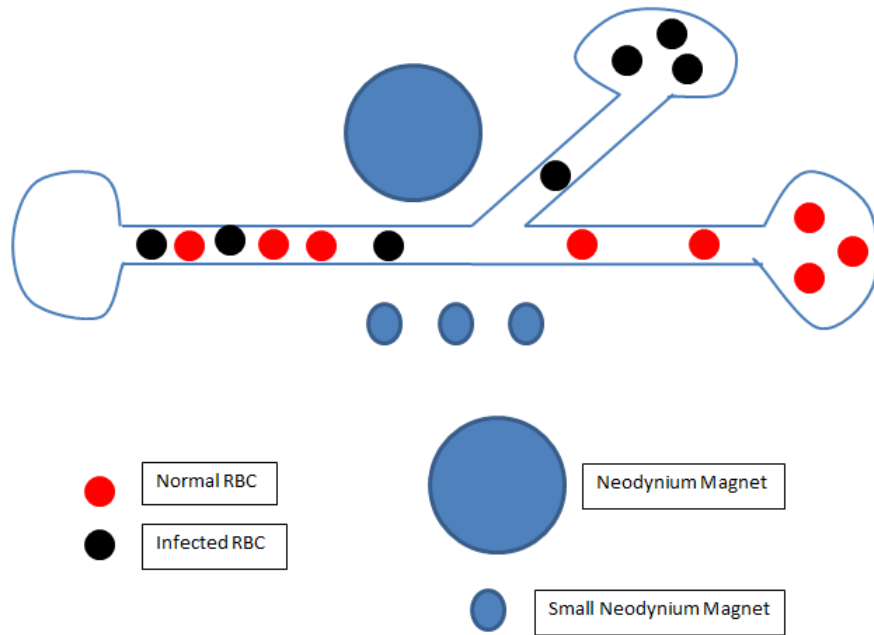


**Figure 3:** This microfluidic device acts in separation of iRBCs from RBCs on the basis of paramagnetic characteristics due to hemozoin.

### C) Separation: Design Idea Three – Electrical

This separation design is based on changes in electrical properties caused to the host RBC upon infection with the malarial parasite. The electrical conductivity of iRBCs is significantly higher than normal RBCs, which allows for electrical separation of these cells. Dielectrophoretic (DEP) forces are non-uniform electric fields that can be created by cells when subject to direct or alternating current. The Differing DEP properties of iRBCs and RBCs contributes to their unique conductivities [8]. These properties can be utilized to separate iRBCs and RBCs in a microfluidic device exposed to properly placed electrical currents. The diagram below illustrates the concept of electrical stimulation in a microfluidic device for the function of separating RBCs (Figure 4). Similar to the magnet separation method, the angle of separation and the placement of the

electrodes could be tested to determine which angle and which placement would lead to the most consistent flow rate and best separation between iRBC and RBCs.

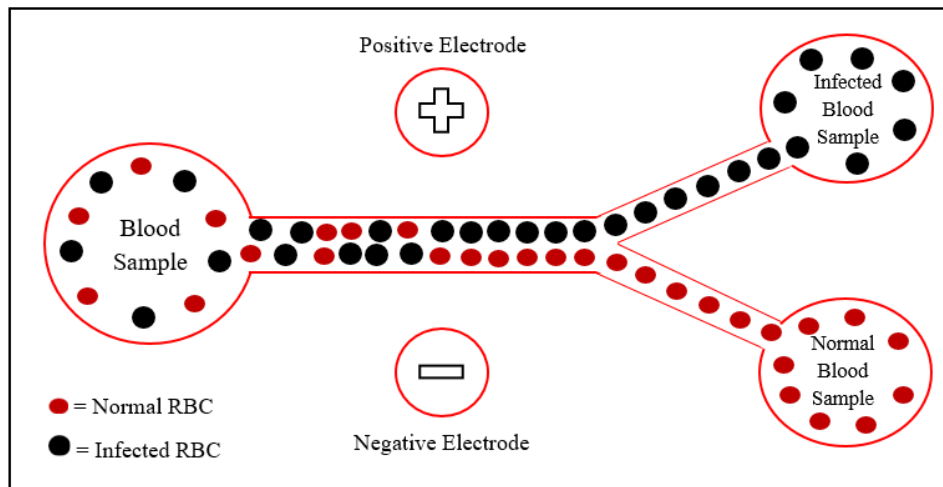


**Figure 4:** This microfluidic device acts in separation of iRBCs from RBCs on the basis of electrical conductivity characteristics.

## Detection Methods

### *D) Detection 1: Design Idea One – BinaxNOW*

BinaxNOW is a currently available diagnostic tool for malaria as described in the introduction section. Its major pitfall is that it requires 5,000 parasites/uL in blood samples for detection, and 5,000 parasites/uL is typically associated with severe stage malaria. The separation techniques described above would act in concentrating the parasites for easier and more successful detection. This assay takes 15 minutes to be completed. By combining BinaxNOW with one of the separation techniques, this tool could become more successful in diagnosing malaria [10].

### *E) Detection 2: Design Idea Two - Polystyrene Beads*

The polystyrene bead method of malaria detection is based on an antigen-antibody interaction in which polystyrene beads are conjugated with an antibody that attaches to an iRBC with antigens specific to that antibody. The beads and iRBCs would then form a visible aggregate in the well, a process known as immunoagglutination [10]. The dried beads could be coated in the well and rehydrated upon use. The aggregation would occur within 2 minutes and would be visible without a microscope [10]. The diagram shown below depicts the polystyrene bead detection design (Figure 5).

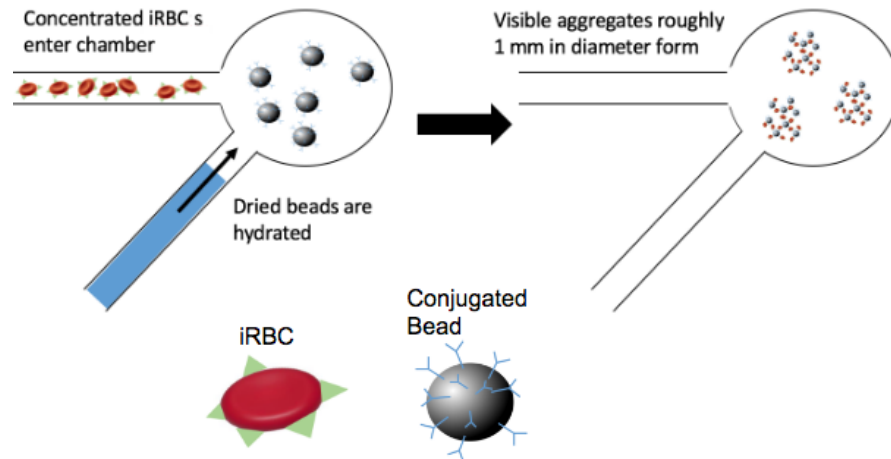


*Figure 5: This detection method occurs through immunoagglutination involving polystyrene beads and iRBCs.*

### *F) Detection 3: Design Idea Three – Gold Nanoparticles*

The gold nanoparticle method of malaria detection is a lateral flow immunoassay (LFIA) whereby iRBCs are detected using unique antigen-antibody interactions. The concentrated blood sample would be placed on the sample pad and then would run down the nitrocellulose paper to pass through the conjugated gold nanoparticle pad. Gold nanoparticles, which are different colors at different diameters, would be conjugated with an antibody specific to iRBC antigens and allow iRBCs to be visualized. The same antibodies present on the gold nanoparticles would also be immobilized on the detection pad. Thus, colored iRBCs would cause a colored line at this junction to signify detection of the specific disease. A conjugated gold nanoparticle for each strain of malaria could be placed in the conjugate pad. Thus, the actual design would contain four separate detection lines, one for each strain of the disease, in addition to the antihuman control line. The antihuman antibody control line would always be detected, if properly functioning, and is present to demonstrate antibody integrity [9]. An image of the gold nanoparticle detection method is outlined below (Figure 6).

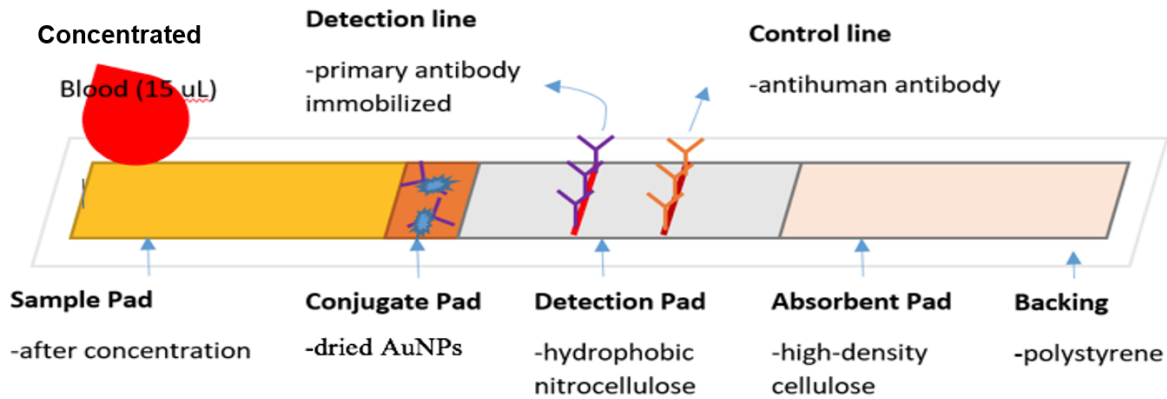


Figure 6. This lateral flow immunoassay detection method occurs through the use of conjugated gold nanoparticles. The colored gold nanoparticles bind to a specific antigen found on iRBCs and are carried along the immunoassay until they reach the designated detection line which immobilizes the antibody found on the gold nanoparticle. This forms a different colored line for each immobilized antibody allowing for the detection of multiple strains of malaria.

### PRELIMINARY DESIGN EVALUATION:

Design	Separation			Detection								
	Cell Deformation	Magnetic Separation	Electric Separation	BinaxNOW	PS Beads	GNPs						
Sensitivity (25)	3	15	5	25	4	20	5	25	4	20	5	25
Equipment Free/Usable in Field/Intuitive (20)	5	20	4	16	3	12	3	12	4	16	5	20
Userfriendly (20)	5	20	5	20	3	12	4	16	4	16	5	20
Time (10)	2	4	4	8	4	8	4	8	5	10	4	8
Cost (10)	5	10	4	8	3	6	1	2	5	10	3	6
Ease of Fabrication (10)	4	8	4	8	3	6	5	10	3	6	2	4
Versatility (type of Malaria or other diseases) (5)	4	4	2	2	2	2	3	3	1	1	5	5
<b>Total</b>	<b>81</b>	<b>87</b>	<b>66</b>	<b>76</b>	<b>79</b>	<b>88</b>						

Figure 7: Decision matrix with criteria in the left column and each design following in two groups of three. The first three designs are separation techniques. The second three designs are detection techniques.

## Design Matrix Evaluation

To evaluate the preliminary designs, they were separated into two categories (figure 7): separation techniques (including cell deformation, magnetic separation, and electric separation) and detection methods (BinaxNOW, polystyrene beads, and gold nanoparticles). It is important to evaluate the designs separately so competing designs can be compared. Improving upon the accuracy of current point of care (POC) devices was deemed the most important, so sensitivity got the highest weight. Another major factor was to produce a device that can be used in rural areas with minimal equipment by untrained technicians. Also, the price and speed of the device should compete with currently available rapid diagnostic tests (RDTs). Lastly, the device should be able to separately detect different strains of malaria for proper treatment of the disease.

The separation techniques all aim to concentrate the iRBCs before analysis. For the separation techniques, sensitivity refers to how specific the separation of iRBCs is; the magnetic separation method scored highest because the magnetic properties of cells are specific to the diseased state. Research has shown that the cell deformation method would separate cells with different surface properties than uninfected RBCs, where diseases such as diabetes would interfere with results [11]. This causes the cell deformation method to receive a lower sensitivity rating than the magnetic and electric methods. To be classified as equipment free and usable in the field, the device must be able to function without a trained technician and should not require a large amount of resources for each test. The cell deformation design scored highest because it would consist solely of a silicon, polydimethylsiloxane (PDMS), that could be manufactured offsite in mass quantities and transported in. The electric separation method scored lowest because it would require batteries and a base with electrodes to be transported to the clinic. To be user friendly the method must be able to concentrate cells without training, so the electric separation method does not pass this test because tuning the electrodes for optimal separation would take constant supervision. Cell deformation scored the lowest for time because the small channels require a low flow rate of liquid that is not as fast as capillary action in the other designs. Lastly, for ease of fabrication, the device must be able to be fabricated and assembled on site. The magnetic separation only had one downfall which was figuring out the placement of the magnets for optimal cell separation. The cell deformation design needed an extremely thin channel, approximately 10  $\mu\text{m}$ , to be made out of PDMS or a plastic like polystyrene, which could pose fabrication problems. The best separation method was deemed to be the magnetic design, as it did the best in four out of six of the criteria and second best in the other two.

The detection methods were evaluated with the same criteria as the separation techniques. Sensitivity is where BinaxNOW is the top performer, this device is 93.5-99.7% sensitive so it is the gold standard in paper based tests. Gold nanoparticles have the possibility to be just as sensitive so they got the same rating, and, for ease of use, this design got the top ranking because it can be read in 15 min by looking for colored lines. The polystyrene bead design is the top performer in time and cost because the test takes two minutes to finish and is made from the cheapest and easiest to assemble materials (except for the preassembled BinaxNOW). The major

drawback of adapting BinaxNOW to the microfluidic device is the cost of about \$40/test. The gold nanoparticles were the chosen detection method to provide the versatility to detect for all four strains of malaria on one test strip. One challenge of this design is the complexity of fabrication, however, this process could be easily be simplified by converting a household printer to lay antibodies on nitrocellulose paper.

### Proposed Final Design

Through the use of our design matrix we decided that the best design combination is the magnetic separation combined with a lateral flow immunoassay using colored gold nanoparticles. This design is a sensitive and easy to use system that can be operated without any training and limited equipment. This system is also cheap enough to compete with current RDTs and has the ability to detect all four strains of malaria.

## **FABRICATION/DEVELOPMENT PROCESS:**

### Materials

The fabrication of each portion of the final prototype required various materials. In order to produce the mask a design was drawn in Adobe Illustrator to scale and sent to FineLine Imaging as a .eps file in order to receive the physical mask. The fabrication of the silicon wafer with the crosslinked photoresist required a silicon wafer, SU-8 50, a spin coater, a UV light for exposure, a hot plate, a developer solution, and acetone. The channels were made of PDMS and required a PDMS base as well as a curing agent. The channels were mounted on a glass slide and plasma treated using a plasma treatment system. The loading wells of the channels were cut out using a metal hole punch.(See Appendix B)

### Methods

In order to pattern the SU-8 photoresist onto the silicon wafer, a mask with the desired negative of the design needs to be made. The mask is a transparent film with a layer of black ink laid down allowing only the desired pattern of light to shine through. The present designs were created in Adobe Illustrator, sent to FineLine Imaging, and printed with 20,320 DPI resolution. (Figure 8). This design has limitations that needed to be taken into account before production. Some of the limitations include leaving space between the designs so the PDMS can be cut for individual analysis of the channels and leaving space near the edges because the photoresist is a consistent height until it comes close to the edge.

The design has a circular loading well that is 5 mm in diameter and connected to a 30 mm long by 100 um wide channel. This long channel splits into two channels separated by 60 degrees that are 100 um wide and 5 mm long. Four different constriction point designs were developed on the mask to test flow rate and potential separation efficiency. The constriction begins 2 mm after the channel begins, lasts for 2 mm, and then slopes back to the full channel

width over the course of 2 mm. The constriction points are 20, 50, 80  $\mu\text{m}$  wide. The 100  $\mu\text{m}$  design does not contain a constriction point as the channel width is 100  $\mu\text{m}$  throughout.

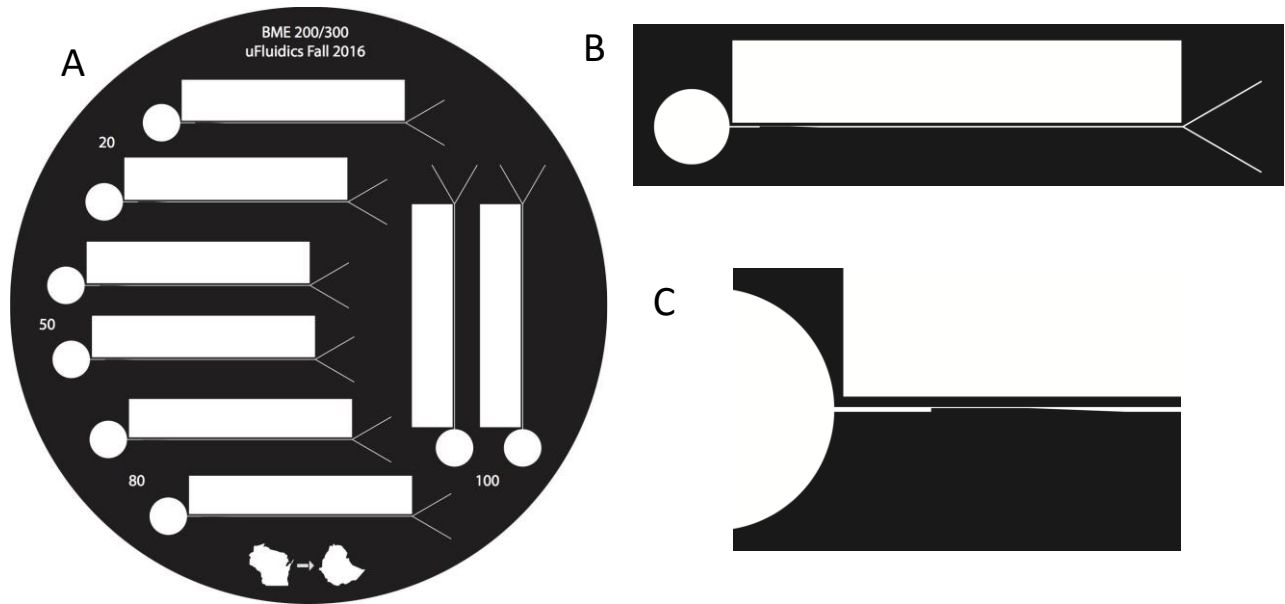


**Figure 8.** *A) Image of the mask designed with the four different channel constriction points outlaid (20, 50, 80, and 100  $\mu\text{m}$ ). There are two replicates of each channel size on the mask. B) Close up of the 20  $\mu\text{m}$  channel constriction point on the mask. C) Enhanced image of the 20  $\mu\text{m}$  constriction point.*

This mask was used to pattern photoresist on a 3" silicon wafer using the method described in Appendix C. First photoresist was spun evenly on the surface (Figure 9), baked and then exposed to UV light to crosslink and bond the 50  $\mu\text{m}$  layer to the wafer (Figure 10). The wafer is then placed in a developer solution to remove all unexposed photoresist. The final wafer is washed with acetone and dried with nitrogen.



**Figure 9:** *A) Picture of the silicon wafer with approximately 3-4 mL of SU-8 50 placed on top. B) Picture of the silicon wafer and SU-8 50 layer post spinning to apply it evenly along the wafer.*

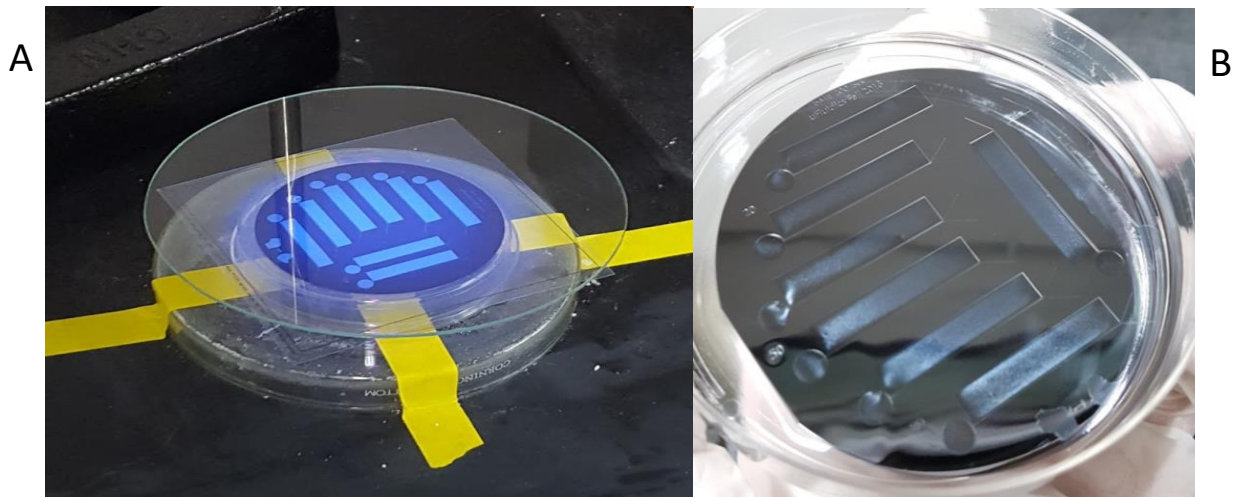


**Figure 10:** A) Picture of mask laid on top of silicon wafer being exposed to UV light for crosslinking of the SU-8. B) Picture of silicon wafer post UV exposure and baking. Fully crosslinked areas visible as outlines of the separate channel designs.

The patterned wafer is now ready for PDMS manufacturing, this fabrication protocol is outlined in Appendix D. The PDMS is mixed and poured over the wafer (Figure 11). This is cured and then the devices are cut from the large slab of silicone.

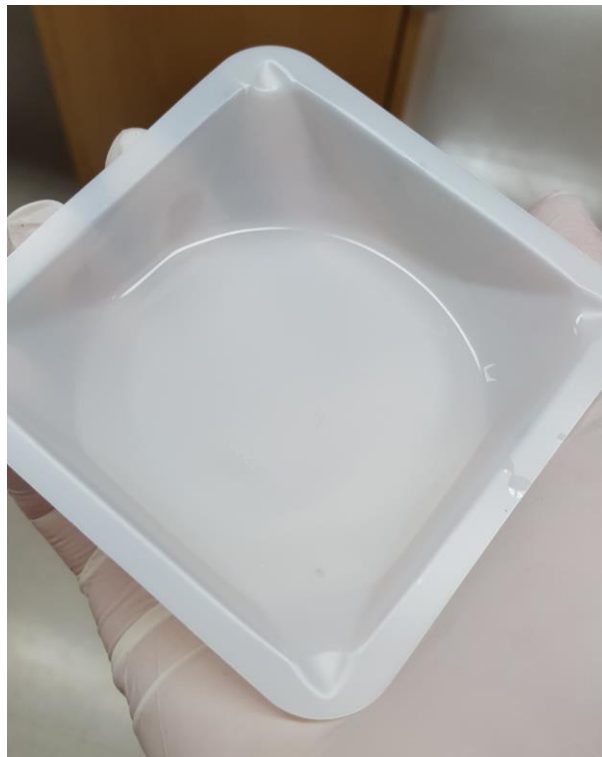


**Figure 11:** Picture of 10:1 (PDMS base : PDMS primer) PDMS from Sylgard Silicone Elastomer Kit post exposure to a vacuum to eliminate the air bubbles from mixing of the PDMS.



**Figure 12:** Picture of the plasma treatment of PDMS channels as well as glass slides.

To prepare the devices for testing they are plasma treated as described in Appendix D, they are then permanently bonded at high temperature and pressure (Figure 13). The holes for inlet and outlet are cut to allow fluid flow.



**Figure 13:** A) Picture of pressure being applied with a weight to permanently bond the PDMS channels to the glass slide after plasma treatment. B) Picture of 6 channels produced after permanent attachment via plasma treatment.

### Final Prototype

The final prototype included both separation and detection components (Figure 14A). The separation portion of the design utilized a 100  $\mu\text{m}$  PDMS microfluidic channel, containing a sample loading portion, constriction point, 3 cm channel length, and diverging point. The detection and separation components were adhered to a glass slide for POC use. The holder was fabricated with high-density polyethylene (HDPE) and a permanently attached 0.6 Tesla magnet was used to consistently house the design and magnet placement (Figure 14B; Appendix F). As the sample is loaded into the starting well, the blood flows through the constriction point, which is intended to modulate the flow rate and homogeneity of blood cells (Figure 14C). Different

constriction point sizes of 20, 50, 80 and 100  $\mu\text{m}$  were tested, which is discussed in the testing/results section below. The final design mechanism is illustrated below (Figure 14D). Conceptually, the blood flows through the channel, the magnet separates the paramagnetic malaria iRBCs and diverges them to the LFIA detection portion of the design. Though the final prototype only included the membrane pad portion of the detection component, the LFIA mechanism is supported in the literature and is still applicable for this design (Appendix E).

Hypothetically, as the blood flows through the conjugate pad portion of the LFIA, the specific antibody conjugated gold nanoparticles rehydrate and bind to the malaria species specific antigens on the surface of the iRBCs. The four malaria species specific antibodies are discussed above in the final design materials section. Assuming the Au-NP concentration is below the saturation point, the now color tagged iRBCs flow down the detection portion of the pad and eventually bind to the same immobilized antibodies on the pad. This binding halts the flow of the iRBCs and allows species specific colored lines to appear as more and more cells bind to the specific immobilized antibodies. If the colored line and control line both appear then the subject tests positive for that specific strain of malaria. A detailed POC use of the device is as follows. Obtain approximately 50  $\mu\text{L}$  of blood sample using a syringe. Load blood into the circular inlet and ensure that sample flows through the channel. Future designs would incorporate a disposable finger prick and allow subjects to place their finger in the circular inlet.

D



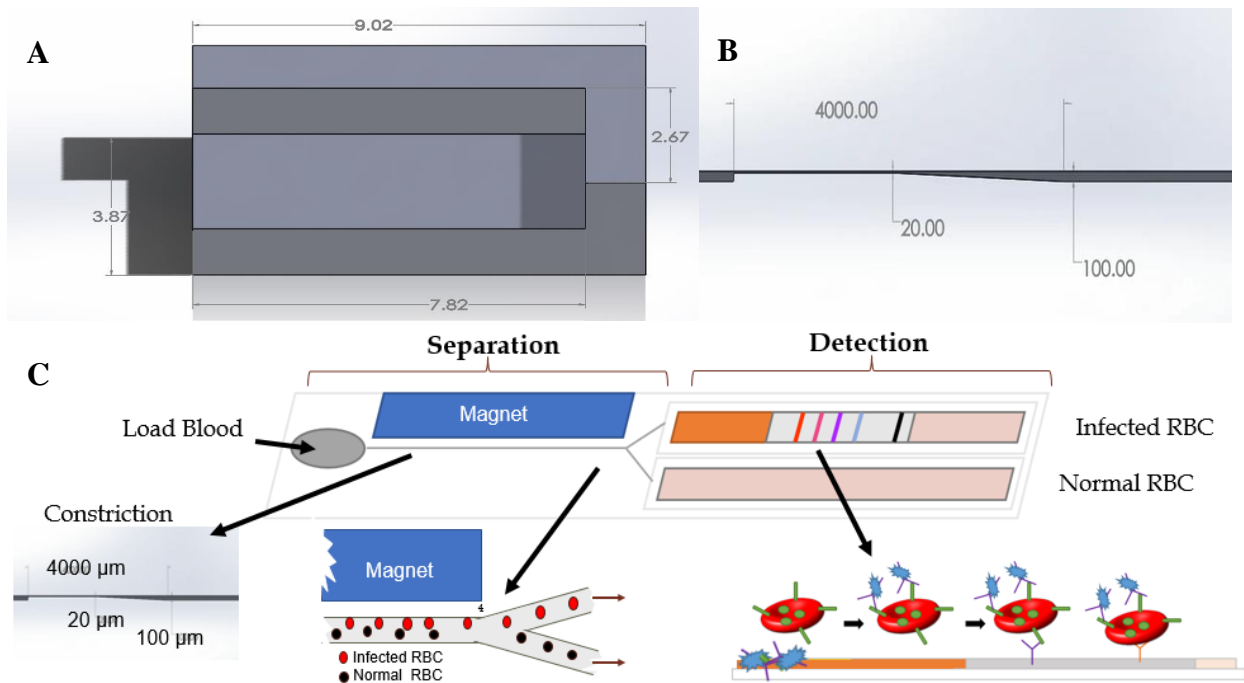


**Figure 14:** **A)** Picture of final prototype. Glass slide device with PDMS microfluidic channel and LFIA pad. Combined with HDPE holder and permanently attached magnet. **B)** Solidworks sketch of final design holder, dimensions in cm. **C)** Solidworks sketch of constriction point, dimensions in  $\mu\text{m}$ . Constriction points tested for design flow: 20, 50, 80, and 100  $\mu\text{m}$ , 20  $\mu\text{m}$  shown. **D)** Final design mechanism.

## Testing

### *Flow Rate Testing:*

Two separate flow rate tests were done in order to gather data on the rate of priming of the channel, as well as the rate of wicking a known volume through the channel. In order to test the priming velocity, the 20, 50, 80 and 100  $\mu\text{m}$  constriction point channels were fabricated and plasma treated onto a glass slide. The loading well was then cut out with a punch for each channel. A pipette was then used to uptake 50  $\mu\text{L}$  of solution, which was then placed in the loading well. The entire well was filled and a slight bubble was created above the channel with 50  $\mu\text{L}$  of solution (Figure 15). The time from when the solution entered the channel to the time when it reached the divergence point was recorded, and the priming velocity was calculated in  $\text{mm}/\text{min}$  (channel length = 30 mm). This process was repeated for all constriction points with a dyed water solution and diluted (25%) porcine blood.

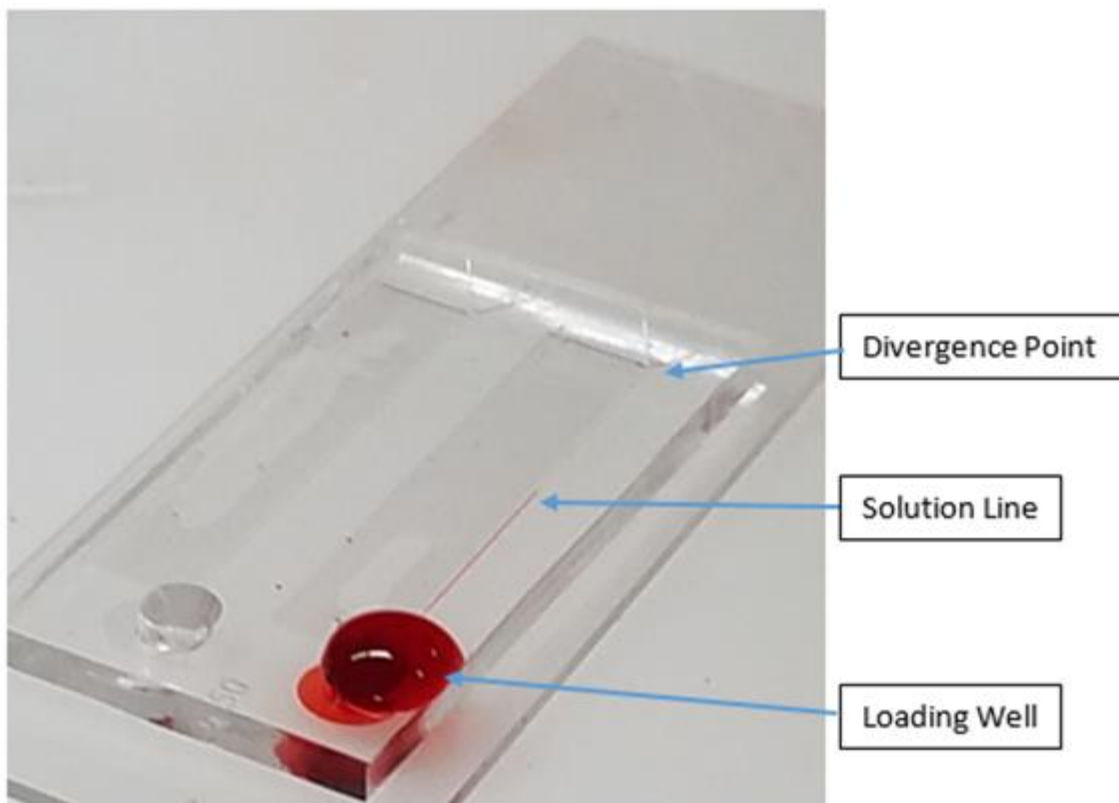


**Figure 15:** Picture of channel priming velocity test on the 50  $\mu\text{m}$  constriction point channel. Outlined are the loading well containing solution, the solution line, and the divergence point where timing measurements were stopped.

The second flow rate test performed was the wicking flow rate test to determine the velocity of the solution through the channel running onto a conjugate LFIA absorbent pad. The same process of fabricating the 20, 50, 80 and 100  $\mu\text{m}$  channels, plasma treating, and cutting out the loading wells were performed for each channel. After the channel had been primed during the previous test, 8.33  $\mu\text{L}$  of solution was placed on the loading well using a micropipette. An absorbent pad was then placed against the channel outlet after the divergence point until it made contact with the solution and began to draw the solution through the channel and onto the pad (Figure 16). The time it took for the bubble of solution to become flush with the PDMS was recorded, as 8.33  $\mu\text{L}$  of solution had then been drawn through the channel. The wicking velocity was then calculated in  $\mu\text{L}/\text{min}$  for each channel constriction size. This process was repeated for all constriction points with both a dyed water solution and diluted (25%) porcine blood.

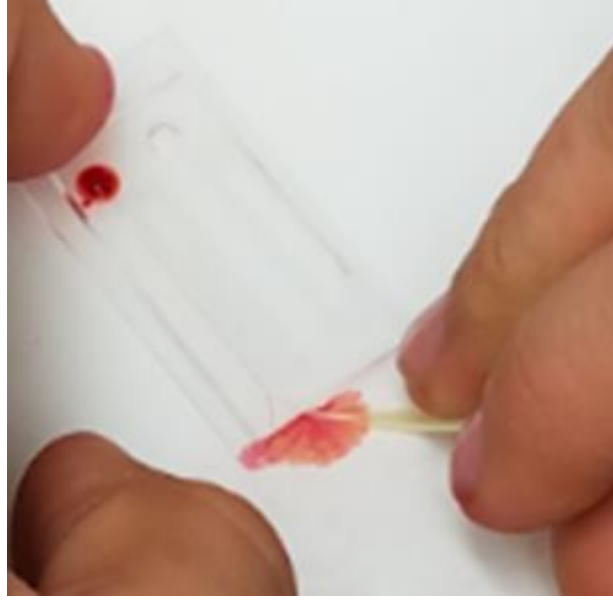


**Figure 16:** Picture of channel wicking velocity test on the 50  $\mu\text{m}$  constriction point channel. Depicted are the loading well containing the water dye solution and the absorbent pad being pressed upon the outlet channels and wicking the solution out of the channel.

### *Magnetic Separation*

In order to test for the magnetic separation capabilities of our device, an assay using ferrofluid suspended in solution was created. A small amount of ferrofluid was placed inside a glass vial containing water and a separate glass vial containing ethanol (Figure 17). The ethanol/ferrofluid mixture was much more separated and easier to visualize where the ferrofluid micelles were located. The ethanol/ferrofluid solution was tested to determine if the magnet was strong enough to pull the ferrofluid out of solution (Figure 18). The ferrofluid/ethanol solution was then placed inside of the loading wells for each of the 20, 50, 80, and 100  $\mu\text{m}$  constriction point channels created. The magnet was placed alongside the channel and the solution drawn through the channel similarly to the process used in the wicking flow rate test. This process was repeated with a sample channel obtained with a width of approximately 1 cm.



**Figure 17:** Picture of the two ferrofluid solutions created for testing. Ferrofluid mixed with ethanol (Left). Ferrofluid mixed with water (Right).



**Figure 18:** Picture of the ferrofluid/ethanol solution in a glass vile. Neodymium magnet placed underneath to draw ferrofluid particles out of solution. Shown to strongly congregate around the magnet.

## RESULTS

### Flow Rate Testing

The testing of the priming velocity yielded data for all of the constriction point replicates, except the 20  $\mu\text{m}$  constriction. The average priming velocity for the dyed water solution (mm/min) for the 50, 80, and 100  $\mu\text{m}$  constriction points were 64.62, 50.57, and 56.56 respectively (Figure 19). None of the priming velocities proved to be statistically significant due to overlapping of error bars. No data was obtained for the channel priming velocity of the diluted porcine blood as positive pressure was needed in order to run the solution to the end of the channel, whereas capillary action guided water down the channel.

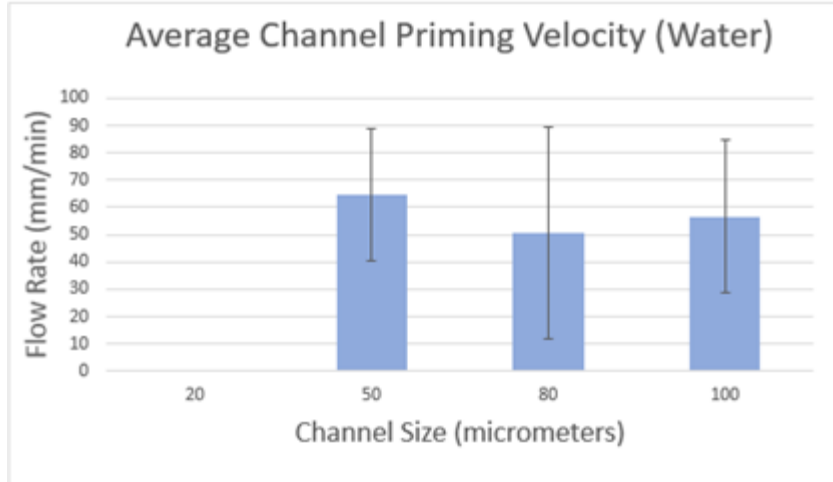


**Figure 19 :** Graph of the average channel priming velocity of the dyed water solution. The channel size in  $\mu\text{m}$  is on the x-axis while the flow rate in  $\text{mm}/\text{min}$  is on the y-axis. The SEM calculated for each are 24.36, 38.8, and 28.0 (Left to right). Each represents  $\pm 1$  SEM.

The testing of the wicking flow rate yielded data for all of the constriction point replicates, except the 20  $\mu\text{m}$  constriction. The average wicking flow rate of the dyed water solution ( $\mu\text{L}/\text{min}$ ) for the 50, 80, and 100  $\mu\text{m}$  constriction points were 2.01, 2.71, and 3.83 respectively (Figure 20). The only statistical significance is the 100 micrometer constriction to the 50 micrometer constriction. The average wicking flow rate of the diluted porcine blood solution ( $\mu\text{L}/\text{min}$ ) for the 50, 80, and 100 micrometer constriction points were 0.99, 1.27, and 1.49 respectively (Figure 21). All of the constriction points were statistically significant from each other.

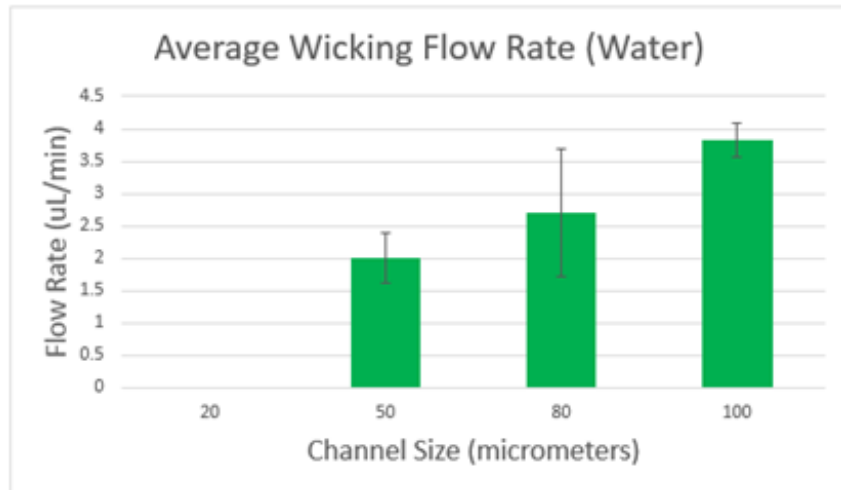


**Figure 20:** Graph of the average wicking flow rate of the dyed water solution. The channel size in  $\mu\text{m}$  is on the x-axis while the flow rate in  $\mu\text{L}/\text{min}$  is on the y-axis. The SEM calculated for each are 0.388, 0.99, and 0.256 (Left to right). Each represents  $\pm 1$  SEM.

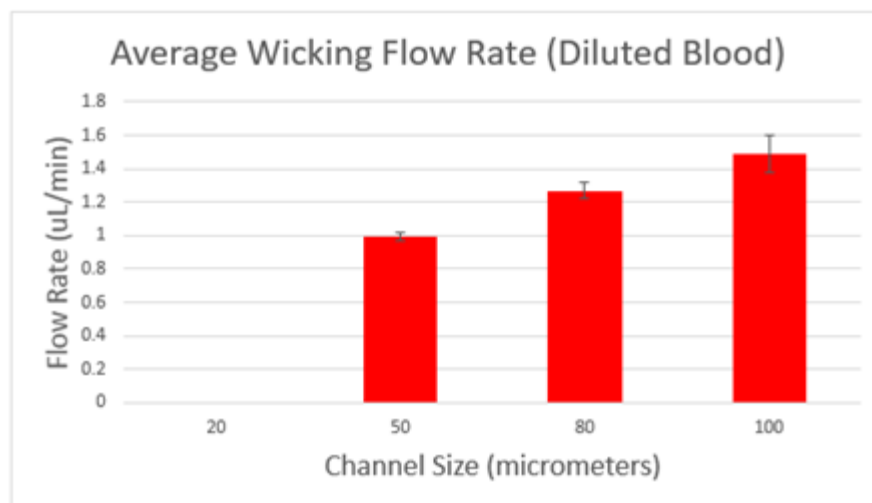


**Figure 21:** Graph of the average wicking flow rate of the diluted porcine blood solution. The channel size in  $\mu\text{m}$  is on the x-axis while the flow rate in  $\mu\text{L}/\text{min}$  is on the y-axis. The SEM calculated for each are 0.026, 0.046, and 0.115 (Left to right). Each represents  $\pm 1$  SEM.

### Magnetic Separation

Upon testing the magnetic separation capabilities of our magnet, it became apparent that the assay created was not a good model for showing how paramagnetic iRBCs would be drawn towards the magnet. The testing using the constriction point channels that were fabricated showed that the ferrofluid particles were too large to pass through the small channel sizes, and the solution could not be run through the channel. The testing using the provided 1cm wide channel allowed the particles to enter the channel, but were immediately drawn towards the wall where the magnet was placed, and remained immobilized there. This showed that the ferrofluid was too strongly magnetized to be used to model the slightly paramagnetic iRBCs. Moving forward, a smaller and weaker paramagnetic particle must be used for proof of concept testing.

### **DISCUSSION**

The preliminary testing of the device with 25% porcine blood showed that the designs with 50, 80 and 100  $\mu\text{m}$  constriction points are feasible for use. However, the channel design with the 20  $\mu\text{m}$  constriction point did not pass water or diluted porcine blood. The design was initially tested with water to measure the channel priming and wicking flow rates. Water flowed through the device passively to prime the channel and to wick onto nitrocellulose paper for the LFIA. The channel priming velocity was highly inconsistent and much faster than the wicking flow rate. The average water wicking flow rates in the functional channels (20  $\mu\text{m}$  - 2.01  $\mu\text{L}/\text{min}$ ; 50  $\mu\text{m}$  - 2.71  $\mu\text{L}/\text{min}$ ; 100  $\mu\text{m}$  - 3.83  $\mu\text{L}/\text{min}$ ) helped to demonstrate how the nitrocellulose paper aided in steadily pulling fluid through the channel at a favorable rate. This was also reinforced by consistently slower average wicking flow rates with 25% porcine blood in these channels (20  $\mu\text{m}$  - 0.99  $\mu\text{L}/\text{min}$ ; 50  $\mu\text{m}$  - 1.27  $\mu\text{L}/\text{min}$ ; 100  $\mu\text{m}$  - 1.49  $\mu\text{L}/\text{min}$ ). However, positive pressure from a pipet was required to prime the channels with the diluted blood prior to passive wicking of the

fluid onto nitrocellulose paper. Because of this requirement, the priming flow rate was not measured for the diluted blood.

The water priming flow rate was highly inconsistent as some channels with the same channel design flowed within 10 seconds, while others took a few minutes. Multiple trials of PDMS channel fabrication were performed, which could contribute to sample variability. However, the 20 second oxygen plasma treatment which reduces PDMS hydrophobicity only lasts for 10 minutes on PDMS [15]. Unfortunately, the design team was unaware of this limitation prior to testing and some fabricated channels were stored and tested as much as 24 hours after plasma treatment. This likely contributed to the substantial variation observed in the water priming flow rate. Although it is expected that this influenced the average wicking flow rate to some extent, this flow rate was quite consistent for water and diluted blood because the rate was primarily dictated by the saturation of the nitrocellulose paper. However, further testing with a new oxygen plasma treatment protocol could yield more consistent results and possibly affect the average wicking flow rate. Protocols described by Hwa Tan *et al* demonstrate that oxygen plasma treatment for 5 minutes and PDMS channel storage in deionized water can cause the enhanced hydrophilicity of the treatment to last for weeks [15]. Furthermore, a more successful oxygen plasma treatment protocol could also allow for the passage of more viscous solutions such as 100% blood. Unfortunately, the design team was not able to pass 50 or 100% blood through the device because all of the channels used for blood testing were plasma treated 24 hours prior to use and the blood was slightly coagulated.

Although 100% blood was not successfully tested, the flow rates observed in the device for diluted porcine blood suggest that the 100  $\mu\text{m}$  constriction size was best for time efficiency of the assay. With this design, it would take approximately 33.6 minutes to run 50  $\mu\text{L}$  of fluid through the channel. However, the 50  $\mu\text{m}$  constriction size only added an additional 17 minutes to come in at 50.6 minutes for assay run time, which is also within the one hour mark that was desired for the POC diagnostic test. Current literature on magnetic cell separation suggests that flow rates of 0.083  $\mu\text{L}/\text{min}$  are successful in separating in 91% of malarial iRBCs in a different design which utilizes a weaker 0.2 Tesla magnet. [16]. Although none of the fabricated designs run quite this slow, this information suggests that 50  $\mu\text{m}$  constriction size may allow for the greatest separation efficiency. An attempt to model the paramagnetic properties of iRBCs was made with the use of ferromagnetic particles in 100% ethanol. However, these particles did not flow through the channels with a magnet present and more paramagnetic beads for testing were not accessible to the design team. Unfortunately, ferromagnetic particles do not accurately model paramagnetic particles as they are much more magnetic and remain strongly magnetized after the removal of a magnetic field [17].

Because several aspects of the design were not successfully tested, a lot of work still needs to be done before the design is finalized. Various observations during testing did prove valuable in evaluating the current design and testing procedures. Redesigning the blood sample addition component to hold the entire blood volume would make the design much easier to use.

It could also be interesting to more accurately control flow rate with the use of a syringe pump and this might prove necessary with future testing. Additionally, it is feasible to predict that the initial portion of the blood sample would be inefficiently separated because the priming flow rate was much faster than the wicking flow rate. In this design, this could potentially be fixed with the use of a buffer as a priming solution to cause blood to only wick through the device. A priming solution could also prove beneficial in rehydration of the dried gold nanoparticles on the nitrocellulose paper. As mentioned previously, testing of the design with a new oxygen plasma treatment could also prove beneficial. However, the true final design would be micromachined from plastic where this would not likely be as much of an issue [18].

In addition to modifications to the current design, more testing and fabrication is required before the concept of this design is proved as a realistic and effective tool for rapid diagnosis of malaria. It would be essential to test the design with malaria infected blood to assess the magnetic separation ability of the magnet and its positioning. Moreover, it would be necessary to begin work on the detection portion of the design, which entails conjugating and drying gold nanoparticles, antibody immobilization, and optimizing long-term storage of the fabricated device. This would also allow for the analysis of the device accuracy with testing of malaria infected blood, which is inevitably one of the most important characteristics of the design. An essential final modification to the design would include better integration of the detection and separation components of the current design to make it a more easily used POC device. Further refining of fabrication protocols for use in Ethiopia would also be useful in making the device more reproducible and accessible (Appendix G).

## **CONCLUSIONS**

The team was tasked with designing a microfluidic device to diagnose and detect malaria in Ethiopia. The proposed final design incorporated components for the separation and detection of malarial iRBCs. Flow rate was assessed in the separation portion of the design; however, future optimization of magnetic separation of iRBCs is still required. The concept of the detection portion of the design has been demonstrated in other industries; however, future determination of the accuracy of the design in detecting the four strains of malaria is also still required. The current results and existing literature suggest that the 50µm channel constriction size would be best because slower flow rate could allow for the greatest cell separation efficiency.

## **ACKNOWLEDGEMENTS**

The design team would like to thank Dr. John Puccinelli and Dr. Christa Wille for all of their advising and shared expertise throughout the semester. We are also thankful to the Biomedical Engineering teaching lab for providing the microfluidic equipment and supplies used for this design. Another thank you goes out to EMD Millipore for providing free LFIA

membrane samples. Finally, we would like to thank Bucky's Butchery for donating the porcine blood used for the device testing.

## REFERENCES

- [1] A. M. Urdea, L. A. Penny, S. S. Olmsted, M. Y. Giovanni, P. Kaspar, A. Shepherd, P. Wilson, C. A. Dahl, S. Buchsbaum, G. Moeller, and D. C. H. Burgess, "Requirements for high impact diagnostics in the developing world."
- [2] World Health Organization, "Malaria," 2016. [Online]. Available: <http://www.who.int/malaria/en/>.
- [3] Center for Disease Control and Prevention, "Malaria," 2016. [Online]. Available: <http://www.cdc.gov/malaria/>.
- [4] L. Syedmoradi, M. Daneshpour, M. Alvandipour, F. A. Gomez, H. Hajghassem, and K. Omidfar, "Biosensors and Bioelectronics Point of care testing : The impact of nanotechnology," vol. 87, pp. 373–387, 2017.
- [5] Alere, "BinaxNOW Malaria," 2016. [Online]. Available: <http://www.alere.com/en/home/product-details/binaxnow-malaria.html>. [Accessed: 10-Jul-2016].
- [6] H. Hou *et al.*, "Deformability based cell margination--a simple microfluidic design for malaria-infected erythrocyte separation," *Lab on a chip.*, vol. 10, no. 19, pp. 2605–13, Aug. 2010. [Online]. Available: <https://www.ncbi.nlm.nih.gov/pubmed/20689864>. Accessed: Oct. 11, 2016.
- [7] A. Trafton and M. N. Office, "A new way to diagnose malaria," MIT News, 2014. [Online]. Available: <http://news.mit.edu/2014/new-method-diagnose-malaria-0831>. Accessed: Oct. 11, 2016.
- [8] W. K. Peng, L. Chen, and J. Han, "Development of miniaturized, portable magnetic resonance relaxometry system for point-of-care medical diagnosis," *Review of Scientific Instruments*, vol. 83, no. 9, p. 95115, Sep. 2012. [Online]. Available: <http://scitation.aip.org/content/aip/journal/rsi/83/9/10.1063/1.4754296>. Accessed: Oct. 14, 2016.
- [9] A. Tay, A. Pavesi, S. R. Yazdi, C. T. Lim, and M. E. Warkiani, "Advances in microfluidics in combating infectious diseases," *Biotechnology Advances*, vol. 34, no. 4, pp. 404–421, Jul. 2016.
- [10] D. Polpanich *et al.* "Detection of malaria infection via latex agglutination assay," *Analytical chemistry.*, vol. 79, no. 12, pp. 4690–5, May 2007. [Online]. Available: <https://www.ncbi.nlm.nih.gov/pubmed/17511424>. Accessed: Oct. 11, 2016.

- [11] G. Tomaiuolo, "Biomechanical properties of red blood cells in health and disease towards microfluidics," vol. 051501, pp. 1–19, 2014.
- [12] J. Friend and L. Yeo, "Fabrication of microfluidic devices using polydimethylsiloxane," vol. 4, no. 2, Mar. 2010. [Online]. Available: <https://www.ncbi.nlm.nih.gov/pmc/articles/PMC2917889/>. Accessed: Oct. 19, 2016.
- [13] A. J. Di Pasqua, R. E. Mishler, Y.-L. Ship, J. C. Dabrowiak, and T. Asefa, "Preparation of antibody-conjugated gold nanoparticles," *Materials Letters*, vol. 63, no. 21, pp. 1876–1879, 2016. [Online]. Available: <http://www.sciencedirect.com/science/article/pii/S0167577X09004194#bib7>. Accessed: Oct. 19, 2016.
- [14] "Photo-assisted inkjet printing of antibodies onto cellulose for the eco2-friendly preparation of immunoassay membranes," *RSC Advances*, vol. 5, no. 38, pp. 29786–29798, Mar. 2015. [Online]. Available: <http://pubs.rsc.org/EN/content/articlepdf/2015/ra/c5ra03442f>. Accessed: Oct. 19, 2016.
- [15] S. H. Tan, N.-T. Nguyen, Y. C. Chua, and T. G. Kang, "Oxygen plasma treatment for reducing hydrophobicity of a sealed polydimethylsiloxane microchannel," *Biomicrofluidics*, vol. 4, no. 3, p. 032204, 2010. [Online]. Available: <https://www.ncbi.nlm.nih.gov/pmc/articles/PMC2967237/>. Accessed: Dec. 11, 2016.
- [16] K.-H. Han and A. B. Frazier, "Paramagnetic capture mode magnetophoretic microseparator for high efficiency blood cell separations," *Lab Chip*, vol. 6, no. 2, pp. 265–273, 2006. [Online]. Available: <http://pubs.rsc.org.ezproxy.library.wisc.edu/en/content/articlepdf/2006/lc/b514539b>. Accessed: Dec. 11, 2016.
- [17] A. Halbreich *et al.*, "Biomedical applications of maghemite ferrofluid," *Biochimie*, vol. 80, no. 5-6, pp. 379–390, May 1998. [Online]. Available: <http://www.sciencedirect.com/science/article/pii/S0300908400800061>. Accessed: Dec. 12, 2016.
- [18] G. Fiorini and D. Chiu, "Disposable microfluidic devices: Fabrication, function, and application," *BioTechniques*, vol. 38, no. 3, pp. 429–446, Mar. 2005. [Online]. Available: [http://www.biotechniques.com/multimedia/archive/00004/BTN\\_A\\_05383RV02\\_O\\_4116a.pdf](http://www.biotechniques.com/multimedia/archive/00004/BTN_A_05383RV02_O_4116a.pdf). Accessed: Dec. 11, 2016.
- [19] Andrysiak P. M, Collins W. E., and Campbell G.H. "Stage-Specific and Species-Specific Antigens of Plasmodium vivax and Plasmodium ovale Defined by Monoclonal Antibodies," *Infection and Immunity*, vol. 54, no. 3, pp. 609-12. Dec. 1986. [Online]. Available: <https://www.ncbi.nlm.nih.gov/pubmed/3536743>

[20] "Nano SU-8," 2002. [Online]. Available: [http://www.microchem.com/pdf/SU8\\_50-100.pdf](http://www.microchem.com/pdf/SU8_50-100.pdf). Accessed: Dec. 14, 2016.

## APPENDIX A

### Product Design Specification-

**Function:** To create a point of care microfluidic device functional in developing countries that can successfully concentrate and diagnose all four strains of malaria via blood chemistry analysis.

#### **Client Requirements:**

- 95% accurate
- Result within one hour
- Battery powered with a battery life of up to 3 hours
- Device needs to be approximately the size of a laptop or smaller
- No more than \$5 per test
- Able to diagnose malaria and distinguish between the strains Plasmodium falciparum and Plasmodium vivax

#### **Design Requirements:**

##### **1. Physical and Operational Characteristics**

- Performance requirements:* The device should accurately diagnose malaria in remote conditions without the use of electricity or advanced laboratory equipment. The device needs to be disposable, ideally give results within an hour and can be used with minimal training.
- Safety:* The device should put the user at a minimal risk for accidental malaria infection via puncture and blood-borne infection.
- Accuracy and Reliability:* Greater than 95% accuracy in detecting all four strains of malaria in a blood sample.
- Life in Service:* The device should be easily discarded after each use to reduce the possibility of transmitting a blood-borne pathogen.
- Shelf Life:* The device should be thermostable and last for up to one year if stored properly.
- Operating Environment:* The device needs to be able to function in outdoor environments experiencing large temperature variations, depending on the season. The device will be used in rural areas, so it should be water and dust resistant.
- Ergonomics:* The device should be easy to recreate without advanced technical knowledge and with minimal laboratory facility requirements.
- Size:* The size of the entire device should be approximately the size of a laptop or smaller.
- Weight:* The weight should be minimal as to increase the ease of which it can be transported to onsite, point of care, locations.
- Materials:* The device must be made with safe and sanitary materials.
- Aesthetics, Appearance, and Finish:* The device should be durable and resistant to normal use by the lab in Ethiopia. Also, it should be able to be shipped in a ready to use form.

## **2. Production Characteristics**

- A. *Quantity*: The creation of at least one functioning device that is able to detect for malaria. The design should be able to be mass produced.
- B. *Target Product Cost*: A test should cost a maximum of \$5.

## **3. Miscellaneous**

- A. *Standards and Specifications*: The device should be greater than 95% accurate, cost less than \$5 per unit, be battery powered (if applicable), and smaller than a laptop. Protocols need to be followed for disposal of the device, so that no blood-borne pathogens are transferred. The design and fabrication should be repeatable, and the device should perform consistently.
- B. *Customer*: This product will be used by technicians in rural areas of Ethiopia to test patients for malaria. The entire diagnosis should take less than an hour, so that treatment can be provided quickly, if needed. The faster the disease is diagnosed and treated, the less fatal the disease becomes.
- C. *Patient-related concerns*: After usage, the device should be able to be easily disposed of in order to not contaminate other patients.
- D. *Competition*: The device cannot infringe on any existing patents or copyrights.
  - a. Binax Now- only brand of malaria rapid diagnostic test approved for use in the United States. Pack of 12 tests sells for \$396.20.
  - b. 86 different malaria rapid diagnostic tests are available from 28 different manufacturers. Cost is \$0.50 to \$1.50 per test, these have no quality control standards and are the currently available method for testing

## Appendix B

### Materials

#### Projected Fabrication of a Single Device

<b>Materials</b>	<b>Price</b>
Fisherbrand Glass Slide	\$0.87
PDMS (one channel)	\$0.25
LFIA Pads (Conjugate, Detection, Absorbent)	\$0.033
Disposable Finger Prick	\$0.08
Antibodies	\$1.00
Gold Nano-particles	\$0.40
Total	\$2.63

#### One Time Costs To Produce One Finished Design

<b>Materials</b>	<b>Price</b>
HDPE Block	\$0.38
Magnet	\$4.77
SU-8 50	\$15.00
Silicon Wafer	\$16.90
Photomask	\$54.00
Total	\$91.05

#### Material Use Throughout the Semester

<b>Materials</b>	<b>Price</b>
------------------	--------------

3 Magnets	\$14.33
Photomask	\$54.00
LFIA Sample Pads	Free (Millipore)
Glass Slides	Free (Lab)
Capillary Tubes	Free (Teaching Lab)
SU-8 (Various)	Free (Teaching Lab)
Silicon Wafer	Free (Teaching Lab)
PDMS	Free (Teaching Lab)
HDPE Block	Free (Teaching Lab)
Ferrofluid	Free (Teaching Lab)
BD Vacutainer	Free (Teaching Lab)
Porcine Blood	Free (Bucky's Butchery)
Chemical Reagents	Free (Teaching Lab)
Total	\$68.33

<b>Material</b>	<b>Product Number</b>	<b>Bulk Price</b>	<b>Single Use Price</b>
HDPE		\$0.38	
Epoxy			
Screws			
Neodymium Magnet		\$4.77	
Glass Slides	Fischer 12-544-4	\$87.00	\$0.87
PDMS Base			\$0.22
PDMS Curing Agent			\$0.03
Silicon Wafer		\$16.90	
Developer Solution			

Acetone			
LFIA Conjugate	Millipore G041	N/A	\$0.01
LFIA Detection	Millipore C	N/A	\$0.01
LFIA Absorbent	Millipore C083	N/A	\$0.01
SU-8 50 MicroChem		\$1500 (est.)	\$15.00
Gold NanoParticles			\$0.40
P. falciparum LDH	BioRad HCA 158	\$210.00	
P. vivax LDH	BioRad HCA 156	\$210.00	
P. ovale MAbs*	N/A	N/A	N/A
Pan P. LDH**	BBI BM355-P42	\$280.57	
Photomask	Order #20272	\$54.00	

\* Developed by [12] and not commercially available

\*\* This is a pan-malaria antibody

## Appendix C

### Silicon Wafer Fabrication

1. Prepare 3" silicon wafer by washing with acetone and then drying with nitrogen. Plasma treat wafer for 30 seconds with the reflective surface facing up.
2. Place wafer on the center of the spin coater chuck and dispense 1" diameter drop of SU-8 50 in the center of the wafer.
3. Spin wafer with an acceleration of 0 to 2000 rpm over 20 seconds and hold at 2000 rpm for 30 seconds. The wafer should now be evenly coated with photoresist 50 um thick.
4. Bake the wafer at 65°C for 5 minutes, then transfer to 95°C for 20 minutes. The photoresist should be sticky but solid at this point due to evaporation of the solvent.
5. Prepare the UV lamp by focusing the light on a circle that is the size of the wafer. Measure the intensity with a light detector to calculate (using the photoresist datasheet) the amount of time necessary to fully crosslink the photoresist [20].
6. Sandwich the mask between the wafer and a thin glass sheet so the desired portions of the photoresist are exposed for the calculated amount of time (Figure 10A).
7. The wafer is baked again at 65°C for 2 minutes and then 95°C for 5 minutes. This hardens and bonds the crosslinked photoresist to the wafer.
8. Cool the wafer and place it in a developer solution while mixing constantly for 8 minutes or until all of the excess photoresist has been removed from the unexposed areas (Figure 10B). This should result in a wafer with the desired features permanently bonded to the surface.
9. A caliper can be used to confirm the features are the correct height. Adjust the time held at 2000 rpm to fix any discrepancy in feature height.

## Appendix D

### PDMS Design Fabrication

1. PDMS is prepared by thoroughly mixing the base and curing agent in a 10:1 weight ratio as described by the directions for the Sylgard Silicone Elastomer Kit (Figure 11). The mixing of these two components creates a lot of air bubbles and thus the mixture is placed in a vacuum until all the bubbles are pulled out of the solution.
2. The wafer with the desired pattern is cleaned with acetone and dried with nitrogen.
3. The PDMS is then poured over the top of the wafer while being careful to not create more air pockets. If bubbles appear, the mixture should be placed in a vacuum until all bubbles rise to the top of the PDMS.
4. The coated wafer is then cured at 100°C for 40 minutes or until the PDMS is firm.
5. After curation at 100°C, PDMS can be carefully peeled from the wafer and cut to separate the features in preparation for bonding. It is important to be careful to not touch the features.
6. Flip the PDMS and glass slides face up (channels up) in the plasma treater and treat for 30 seconds (Figure 12).
7. Immediately after treatment the PDMS and glass slides are pressed together by hand and bonded at 100°C for 10 minutes with a constant pressure (Figure 13).
8. The testable device is then made by punching holes in the inlet and cutting openings for the exit channels.

## Appendix E

### LFIA Fabrication

1. Take glass slide with attached PDMS microfluidics separation device and clean with ethanol soaked kimwipe
2. Acquire the membrane pads and cut the pads shape with ethanol sanitized scissors
  - LFIA
    - Conjugate Pad: .5 cm x .5 cm
    - Detection Pad: 2.5 cm x .5 cm
    - Absorbent Pad: 1 cm x .5 cm
  - Mirrored Waste Pad
    - Absorbent Pad: 4 cm x .5 cm
3. With pad adhesive, construct the LFIA and mirror absorbent pad.
  - LFIA order: Conjugate Pad, Detection Pad, Absorbent Pad
  - Leave 1 mm overhang.
4. Attach to glass slide with the other side of the adhesive, weaving the overhang under the corresponding channel, top most being the LFIA portion.
5. Attach half of a glass slide over the pads via command strip to prevent open blood exposure.

## Appendix F

### Product Holder Fabrication

1. Acquire a bulk piece of HDPE
2. Measure and cut out on a band saw three pieces of HDPE
  - Block 1- 9.02 cm x 3.87 cm
  - Block 2- 9.02 cm x 1.2 cm
  - Block 3- 2.67 cm x 1.2 cm
3. Stack blocks 2 and 3 on block 1 forming an “L” shape
4. Once the blocks are in position with the outer edges flush, drill a hole in the center of block 3, extending approximately halfway into block 1
  - Hole center is at 1.335 cm in the X direction and 0.6 cm in the Y direction
5. Drill two holes in block 2 at the positions  $\frac{1}{3}$  and  $\frac{2}{3}$  of length
  - Hole centers both at 0.6 cm in the Y direction and at 3.01 cm and 6.02 cm in the X direction
6. Countersink the holes of blocks 2 and 3 to depth that leaves the screws flush with surface
7. Screw blocks 2 and 3 into block 1
8. Epoxy the neodymium magnet 1 mm above the top surface of block 1 and approximately 1 cm from the end opposite of block 3

## Appendix G

### Future Design Development in Ethiopia

Though the final prototype only included the microfluidic separation portion of the design, the detection concepts are still valid. The LFIA membrane pad portion of the device was included in the prototype to provide initial context of the separation method. The following published articles can be used in future development of the product and fabrication of the detect method.

#### Gold Nanoparticle Antibody Conjugation

- <https://www.innovabiosciences.com/gold-conjugation-kits.html>

#### Gold Nanoparticle Dehydration

- [https://www.tedpella.com/gold\\_html/gold-tec.htm](https://www.tedpella.com/gold_html/gold-tec.htm)

#### Antibody Immobilization on Diagnostic Pad

- [http://www.emdmillipore.com/US/en/products/ivd-oem-materials-reagents/lateral-flow-membranes/n6mb.qB.L0YAAAE\\_gut3.Lxi.nav](http://www.emdmillipore.com/US/en/products/ivd-oem-materials-reagents/lateral-flow-membranes/n6mb.qB.L0YAAAE_gut3.Lxi.nav)